

We are IntechOpen, the world's leading publisher of Open Access books Built by scientists, for scientists

6,900

Open access books available

186,000

International authors and editors

200M

Downloads

Our authors are among the

154

Countries delivered to

TOP 1%

most cited scientists

12.2%

Contributors from top 500 universities



WEB OF SCIENCE™

Selection of our books indexed in the Book Citation Index
in Web of Science™ Core Collection (BKCI)

Interested in publishing with us?
Contact book.department@intechopen.com

Numbers displayed above are based on latest data collected.
For more information visit www.intechopen.com



Cooperative Communication over Multi-Scale and Multi-Lag Wireless Channels

H. Lu, T. Xu and H. Nikookar

Additional information is available at the end of the chapter

<http://dx.doi.org/10.5772/48719>

1. Introduction

The development of wireless communication applications in the last few years is unprecedented. Wireless communication has evolved in various ways. The next generation of wireless systems should service more users while supporting mobility and high data rates. These requirements necessitate efficient use of available resources to provide acceptable service quality.

In the wireless channel, fading can be coped with by using diversity techniques or by transmitting the signal over several independently fading channels and combining different signal at the receiver before demodulation and detection. Spatial diversity techniques are known to increase the system reliability without sacrificing time and bandwidth efficiency. However, due to the limitation of the diversity order and correlated channel, multiple antenna diversity is not always practically feasible.

Spatial diversity has been studied intensively in the context of Multiple-Input-Multiple-Output (MIMO) systems [1]. It has been shown that utilizing MIMO systems can significantly improve the system throughput and reliability [2]. However, MIMO gains hinge on the independence of the paths between transmit and receive antennas, for which one must guarantee antenna element separation several times the wavelength, a requirement difficult to meet with the small-size terminals. To overcome this problem, and to benefit from the performance enhanced by MIMO systems, cooperative diversity schemes for the relay transmission have been introduced in [3-5].

Cooperative diversity [6] is an alternative way to achieve spatial diversity when the multiple antenna structure is not an option. Cooperative communications offer diversity based on the fact that other users in the cooperative network are able to overhear the transmitted signal and forward the information to the destination through different paths. Cooperative

communications have been receiving a lot of attention recently as an attractive way to combat frequency-selectivity of wireless channel, as they consume neither time nor frequency resources. Furthermore, cooperative communications are promising techniques to increase the transmission reliability, since they can achieve spatial diversity by using the relay nodes as virtual antennas, and mitigating fading effects. By adopting relay to forward information, we can increase the capacity, lower the bit-error rate, and increase the achievable transmission range.

There are mainly two relaying protocols in cooperative communications: Amplify-and-Forward (AF) and Decode-and-Forward (DF). In AF, the received signal is amplified and retransmitted to the destination. The advantage of this protocol is its simplicity and low cost implementation. However, the noise is also amplified at the relay. In the DF, the relay attempts to decode the received signals. If successful, it re-encodes the information and retransmits it. Therefore, DF relaying usually enjoys a better transmission performance than the AF relaying. The time-consuming decoding tradeoff for a better cooperative transmission, and finding the optimum hybrid cooperative schemes, that include both DF and AF for different situations, is an important issue for the cooperative networks design.

In this chapter, we investigate the performance and relay selection issue in cooperative wideband communication systems. Wideband communication systems are defined as having a fractional bandwidth—the ratio of single-sided bandwidth to center frequency—that exceeds 0.2 [7]. Wideband channels are of interest in a variety of wireless communication scenarios including underwater acoustic systems and wideband terrestrial radio frequency systems such as spread-spectrum or ultra wideband. Due to the nature of wideband propagation, such channels exhibit some fundamental differences relative to so-called narrowband channels. In the wideband systems, the effects of mobility in the multipath mobile environment are not well described by frequency-domain spreading, but rather by time-domain scale spreading. More specifically, in narrowband channels, the transmitted signal experiences multiple propagation paths each with a possibly distinct Doppler frequency shift, and thus these channels are also known as multi-Doppler shift, multi-lag channels. For wideband channels, on the other hand, each propagation path experiences a distinct Doppler scale, hence the term, multi-scale, multi-lag channel. For both types of wideband and narrowband time-varying channels, so-called canonical channel models have been proposed [8-11], limiting the number of channel coefficients required to represent the channel.

In particular, there has been significant success in the application of canonical models to narrowband time-varying channels [8]. For wideband time-varying channels a canonical model has been proposed in [9-11], which is also dubbed as the scale-lag canonical model. This model has been adopted for direct sequence spread spectrum (DSSS) communication systems [11] to develop a scale-lag RAKE receiver to collect the diversity inherent in the multi-scale multi-lag channel. In addition, this model has spurred the use of wavelet signaling due to the fact that when the wavelets are “matched” to the scale-lag model, the receiver structure is greatly simplified – the signals corresponding to different scale-lag

branches of the model are orthogonal when a single wavelet pulse is transmitted. The single pulse case is examined in paper [10]. Multi-scale multi-lag wavelet signaling is possible as well [12], [13], although inter-scale and inter-delay interference results. In paper [12], multiple receiver designs to combat such interference are provided exploiting the banded nature of the resulting interference.

Note that scale-spreading arises from the same fundamental mechanism that causes Doppler spreading. This scale-lag diversity is better described by the wavelet transform than the conventional time-frequency representation for the narrowband linear time-varying (LTV) system, and is so called the wideband LTV representation [10, 11]. Wideband LTV representation has been proven and verified for many applications in terms of high data rate wireless communications [14-17], high-speed underwater acoustic communications [18-20], vehicle-to-vehicle (V2V) wideband communication systems [21, 22], and radar/sonar systems [23]. In general, the transmit waveform could be designed to optimally enable the scale-lag diversity in the wideband LTV system.

Doppler scaling and multipath spread in the wideband system implementations are usually treated as distortions rather than potential diversity sources, and always compensated after estimation. In this chapter, Doppler scaling and multipath spread are utilized to obtain a joint scale-lag diversity with the discrete multi-scale and multi-lag wireless channel model by properly designing signaling and reception schemes using the discrete wavelet transform. The wavelet technique used in the wideband system is well motivated since wideband processing is intimately related to the wavelet theory [24-26]. The wideband LTV representation has proven useful in many applications as noted above. However, no cooperative wavelet implementations have been exploited to provide further increased performance for wideband systems.

In this chapter, we will design a cooperative wavelet communication scheme to exploit the joint scale-lag diversity in the wideband LTV system. Furthermore, we propose the analytical Bit Error Rate (BER) expression for the cooperative wideband system, and provide a dynamic optimal selection strategy for relay selection to gain from multi-relay, multi-scaling, and multi-lag diversity, and maximize the whole system transmission performance.

The rest of chapter is organized as follows. In section 2, an overview of the multi-scale and multi-lag diversity in wideband system is provided. In section 3, we investigate the general hybrid cooperative scheme that includes both DF and AF relays, and review the SNR thresholding scheme as well as dynamic optimal combination strategy for the hybrid DF-AF cooperation to achieve the optimal system BER performance. In section 4, we construct the cooperative wavelet wideband transmission strategy, and derive the analytical BER expression for the cooperative wavelet communications in the multi-relay, multi-scale and multi-lag channel. In Section 5, we represent the dynamic optimal selection strategy for the relay selection. Simulations results are provided in Section 6 and are compared to the analytical formulas. The relay selection is also illustrated in this section. Finally, Section 7 concludes the chapter.

2. Wideband multi-scale and multi-lag representation

Multi-scale and multi-lag representation is suitable for the wideband systems to satisfy either of the two conditions, i.e., absolute condition or relative condition. First is the absolute condition, which requires the signal fractional bandwidth (ratio of bandwidth to center frequency) to be larger than 0.2. Second one is the relative condition, i.e., the motion velocity v , the propagation speed c and the signal time bandwidth (TB) product should satisfy $2v/c \gg 1/(TW)$, where T stands for the transmitted signal duration and W denotes the transmitted signal bandwidth. Therefore, the multi-scale and multi-lag system can be defined as a system that operates at high fractional bandwidths or large TB products or when the v/c ratio is large.

For example, an ultra wideband (UWB) system transmits signals with high fractional bandwidths (> 0.2) or large TB products (10^5 - 10^6) to improve resolution capacity and increase noise immunity [27]. Or an underwater acoustic environment with fast moving objects could result in a large ratio due to the relatively low speed of sound [28]. In these situations, multi-scale and multi-lag representation is needed to account for the Doppler scale effects, but not Doppler shift.

Under the wideband background mentioned above, we consider a multi-scale and multi-lag system, that is, a signal, $x(t)$, transmitted over a wideband propagation medium is received as

$$y(t) = \int_{A_l}^{A_u} \int_0^{T_d} h(\tau, a) \sqrt{a} x(a(t - \tau)) d\tau da + n(t), \quad (1)$$

where $a \approx 1 + 2v/c$ is the Doppler scale, results in a time compression or expansion of the waveform caused by a relative velocity v between transmitter and scatterer. When the Doppler scale is such that $a > 1$, then the scatterer is approaching the transmitter and the transmitted signal is compressed with respect to time; in contrast, when $0 < a < 1$, the received signal is dilated and the scatterer is moving away from the transmitter. τ is the propagation delay due to reflections of $x(t)$ by scatterers in the medium. Channel gain $h(\tau, a)$ can be modeled as a stochastic process, when the system is randomly varying [10]. Due to physical restrictions on the system, we can assume that $h(\tau, a)$ is effectively nonzero only when $0 < A_l \leq a \leq A_u$ and $0 \leq \tau \leq T_d$, where $A_u - A_l$ is the Doppler scale spread and T_d is the multipath delay spread. The noise process, $n(t)$ is modeled as a white Gaussian random process.

Note that regardless the noise term, Eq. (1) is in the form of an inverse wavelet transform with $x(t)$ acting as the wavelet. Therefore, according to the wavelet theory, we sample the multi-scale and multi-lag plane in a dyadic lattice as shown in Fig. 1 [10, 29].

Without loss the generality, we consider BPSK modulation, the information-bearing symbol of the transmitted signal is $b_0 = \pm 1$. From the multi-scale and multi-lag channel defined in Fig. 1, the overall baseband signal at the receiver can be rewritten as:

$$y(t) = b_0 \sum_{m=M_0}^{M_1} \sum_{l=1}^{L(m)} h(m,l) \sqrt{2^m} x\left(2^m t - \frac{l}{W}\right) + n(t), \quad (2)$$

where $L(m)$ denotes the number of the multilag for corresponding scaling index m , as shown to be the number of cross points on each row in Fig. 1. M_0 and M_1 are lower and upper bounds of m , respectively. In fact, the multilag resolution in a wideband channel is $1/(aW)$ if the signal is scaled by a . When the number of scatterers contributing to the discrete channel gain $h(m,l)$ is exceedingly large, the random variables $h(m,l)$ can be assumed Gaussian and therefore independent.

Consequently, the inverse discrete wavelet transform description in Eq. (2) effectively decomposes the wideband channel into

$$M = \sum_{m=M_0}^{M_1} (L(m)), \quad (3)$$

orthogonal, flat-fading channels. This results in a potential joint scale-lag diversity order M that can be exploited to increase system performance.

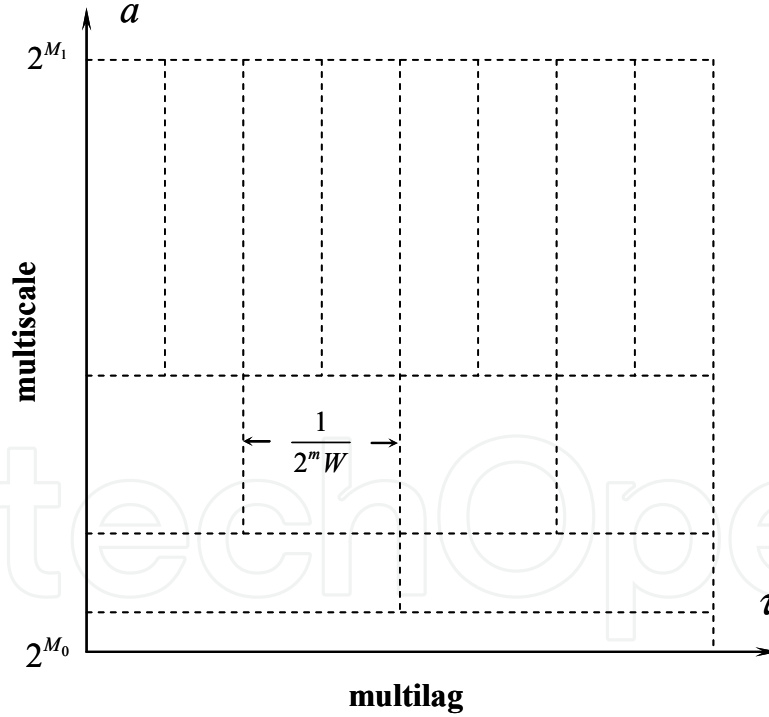


Figure 1. Dyadic sampling in the multi-scale and multi-lag plane, the dyadic scale is $a = 2^m$ and for the given $M_0 \leq m \leq M_1$, m, M_0, M_1 are all integer. The multi-lag resolution is $1/(2^m W)$, given the signal bandwidth W .

In order for a scale-lag RAKE receiver to collect the aforementioned diversity components, transmitted signal should be designed as a wavelet-based waveform. Wideband multi-scale and multi-lag channel performs the inverse discrete wavelet transform on the transmitted

signal $x_{m,l}(t)$. At the receiver side, for the diversity component corresponding to the m -th scale and l -th lag, the detection statistic

$$\lambda_{m,l} = \left\langle y(t), \sqrt{2^m} x \left(2^m t - \frac{l}{W} \right) \right\rangle = \int_{-\infty}^{\infty} y(t) \sqrt{2^m} x^* \left(2^m t - \frac{l}{W} \right) dt \quad (4)$$

is the correlator output of the received signal $y(t)$ and the basic waveform $\sqrt{2^m} x(2^m t - l/W)$. Therefore, the detection statistic $\lambda_{m,l}$ can be obtained by the dyadic scale-lag samples of the discrete wavelet transform of $y(t)$ associated with the wavelet function $x(t)$, which forms a scale-lag RAKE receiver. Then, the channel gain is combined coherently to obtain the estimate of the transmitted information symbol b_0 as

$$\hat{b}_0 = \text{sign} \left\{ \text{Re} \left(\sum_{m=M_0}^{M_1} \sum_{l=1}^{L(m)} h^*(m,l) \lambda_{m,l} \right) \right\}. \quad (5)$$

We note that this coherent detection of the scale-lag RAKE receiver corresponds to a Maximum Ratio Combination (MRC).

Wideband LTV multi-scale and multi-lag channels are of interest in a variety of wireless communication scenarios including wideband terrestrial radio frequency systems such as spread-spectrum systems or Ultra Wideband (UWB) systems and underwater acoustic systems. Due to the nature of wideband propagation, such wideband multi-scale and multi-lag channels exhibit some fundamental differences compared to the so-called narrowband channels. In particular, these multi-scale, multi-lag channel descriptions offer improved modeling of LTV wideband channels over multi-Doppler-shift, multi-lag models [10-12]. Orthogonal Frequency Division Multiplexing (OFDM) technology has been introduced and examined for wideband LTV channels. Approaches include splitting the wideband LTV channel into parallel narrowband LTV channels [30] or assuming a simplified model which reduces the wideband LTV channel to a narrowband LTV channel with a carrier frequency offset [31].

Receivers for single-scaled wavelet-based pulses for wideband multi-scale, multi-lag channels are presented in [10, 11], and a similar waveform is adopted in spread-spectrum systems [32] over wideband channels modeled by wavelet transforms; while [33] considers equalizers for block transmissions in wideband multi-scale, multi-lag channels. In order to achieve better realistic channel matching, single-scaled rational wavelet modulation was designed in [34]. The above mentioned schemes all employ single-scale modulation and thus do not maximize the spectral efficiency. In order to exploit the frequency diversity, a new form of Orthogonal Wavelet Division Multiplexing (OWDM) has been previously examined in [35] for additive white Gaussian noise channels.

However, no cooperative schemes for multi-scale, multi-lag channels have been exploited to provide further increased performance for wideband systems. In this chapter, we will design a cooperative wavelet communication scheme to exploit the joint scale-lag diversity

in the wideband LTV system. Furthermore, we propose the analytical BER expression for the cooperative wideband system, and provide a dynamic optimal selection strategy for relay selection to gain from multi-relay, multi-scaling, and multi-lag diversity, and maximize the whole system transmission performance.

3. Cooperative DF and AF relay communication

3.1. Cooperative DF/AF system model

In the cooperative communications system, DF relaying performs better than AF relaying, due to reducing the effects of noise and interference at the fully decoding relay. However, in some case, DF relaying entails the possibility of forwarding erroneously detected signals to the destination as well; causing error propagation that can diminish the performance of the system. The mutual information between the source and the destination is limited by the mutual information of the weakest link between the source-relay and the combined channel from the source-destination and relay-destination.

Since the reliable decoding is not always available, which also means DF protocol is not always suitable for all relaying situations. The tradeoff between the time-consuming decoding, and a better cooperative transmission, finding the appropriate hybrid cooperative schemes, which include both DF and AF for specific situations, is a critical issue for the cooperative relaying networks design.

In this Section, we review the cooperative strategy with the combination of the DF and AF relay as shown in Fig. 2, where we transmit data from source node S to destination node D through R relays, without the direct link between S and D . This relay structure is called 2-hop relay system, i.e., first hop from source node to relay, and second hop from relay to destination. The channel fading for different links are assumed to be identical and statistically independent, quasi-statistic, i.e., channels are constant within several symbol durations. This is a reasonable assumption as the relays are usually spatially well separated and in a slow changing environment. We assume that the channels are well known at the corresponding receiver sides, and a one bit feedback channel from destination to relay is used for removing the unsuitable AF relays. All the Additive White Gaussian Noise (AWGN) terms have equal variance N_0 . Relays are re-ordered according to the descending order of the Signal-to-Noise Ratio (SNR) between S and Q , i.e., $\text{SNR}_{SQ_1} > \dots > \text{SNR}_{SQ_R}$, where SNR_{SQ_r} denotes the r -th largest SNR between S and Q .

In this model, relays can determine whether the received signals are decoded correctly or not, just simply by comparing the SNR to the threshold, which will be elaborated in Section 3.2. Therefore, the relays with SNR above the threshold will be chosen to decode and forward the data to the destination, as shown with the white hexagons in Fig. 2. The white circle is the removed AF relay according to the dynamic optimal combination strategy which will be described in Section 3.3. The rest of the relays follow the AF protocol, as shown with the white hexagons in Fig. 2 [36].

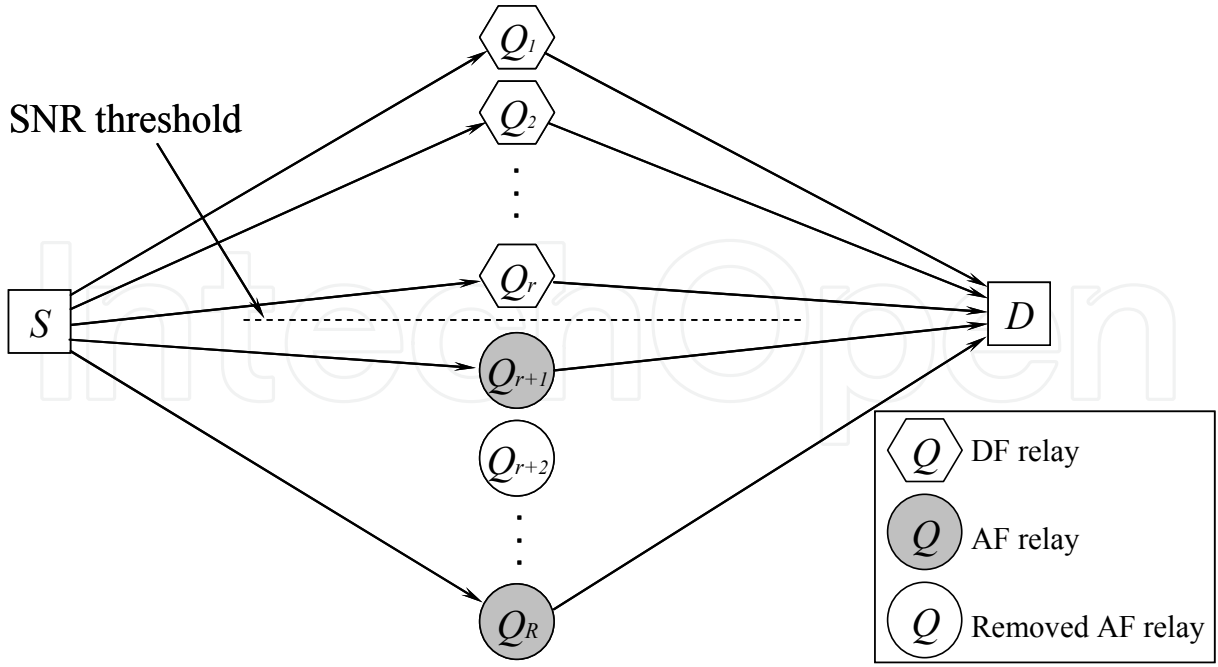


Figure 2. Cooperation communications with dynamic optimal combination of DF/AF relays (S : Source, D : Destination, Q_r : r -th Relay)

The received SNR at the destination in the hybrid cooperative network can be denoted as

$$\gamma_h = \sum_{Q_i \in \text{DF}} \frac{E_Q h_{Q_i, D}}{N_0} + \sum_{Q_j \in \text{AF}} \frac{\frac{E_S h_{S, Q_j}}{N_0} \frac{E_Q h_{Q_j, D}}{N_0}}{\frac{E_S h_{S, Q_j}}{N_0} + \frac{E_Q h_{Q_j, D}}{N_0} + 1}, \quad (6)$$

where $h_{Q_i, D}$, h_{S, Q_j} and $h_{Q_j, D}$ denote the power gains of the channel from the i -th relay to the destination in DF protocol, source node to the j -th relay in AF protocol and j -th relay to the destination in AF protocol, respectively. E_S and E_Q in Eq. (6) are the average transmission energy at the source node and at the relays, respectively. By choosing the amplification factor A_{Q_j} in the AF protocol as

$$A_{Q_j}^2 = \frac{E_S}{E_S h_{S, Q_j} + N_0}, \quad (7)$$

and forcing the E_Q in DF equal to E_S , it will be convenient to maintain constant average transmission energy at relays, equal to the original transmitted energy at the source node.

The receiver at the destination collects the data from DF and AF relays with a MRC. Because of the amplification in the intermediate stage in the AF protocol, the overall channel gain of the AF protocol should include the source to relay, relay to destination channels gains and amplification factor. The decision variable u at the MRC output is given by

$$u = \sum_{Q_i \in \text{DF}} \frac{(H_{Q_i,D})^* Y_{Q_i}}{(H_{Q_i,D})^* H_{Q_i,D}} + \sum_{Q_j \in \text{AF}} \frac{(H_{S,Q_j} A_{Q_j} H_{Q_j,D})^* Y_{Q_j}}{(H_{S,Q_j} A_{Q_j} H_{Q_j,D})^* (H_{S,Q_j} A_{Q_j} H_{Q_j,D})}, \quad (8)$$

where Y_{Q_i} and Y_{Q_j} are the received signal from DF i -th relay and AF j -th relays, respectively, and $(\cdot)^*$ denotes the conjugate operation. $H_{Q_i,D}$, H_{S,Q_j} and $H_{Q_j,D}$ are frequency response of the channel power gains, respectively.

In the hybrid DF/AF cooperative network, DF plays a dominant role in the whole system. However, switching to AF scheme for the relay nodes with SNR below the threshold often improves the total transmission performance, and accordingly AF plays a positive compensating role.

3.2. SNR thresholding scheme for DF relays Cooperative DF/AF system model

In general, mutual information I is the upper bound of the target rate B bit/s/Hz, i.e., the spectral efficiency attempted by the transmitting terminal. Normally, $B \leq I$, and the case $B > I$ is known as the outage event. Meanwhile, channel capacity, C , is also regarded as the maximum achievable spectral efficiency, i.e., $B \leq C$.

Conventionally, the maximum average mutual information of the direct transmission between source and destination, i.e., I_D , achieved by independent and identically distributed (i.i.d) zero-mean, circularly symmetric complex Gaussian inputs, is given by

$$I_D = \log_2(1 + \text{SNR } h_{S,D}), \quad (9)$$

as a function of the power gain over source and destination, $h_{S,D}$. According to the inequality $B \leq I$, we can derive the SNR threshold for the full decoding as

$$\text{SNR} \geq \frac{2^B - 1}{h_{S,D}}. \quad (10)$$

Then, we suppose all of the X relays adopt the DF cooperative transmission without direct transmission. The maximum average mutual information for DF cooperation I_{DF_co} is shown [3] to be

$$I_{DF_co} = \frac{1}{X} \min \left\{ \log_2 \left(1 + \sum_{r=1}^R \text{SNR } h_{S,Q_r} \right), \log_2 \left(1 + \sum_{r=1}^R \text{SNR } h_{Q_r,D} \right) \right\}, \quad (11)$$

which is a function of the channel power gains. Here, R denotes the number of the relays.

For the r -th DF link, requiring both the relay and destination to decode perfectly, the maximum average mutual information I_{DF_li} can be shown as

$$I_{DF_li} = \min \left\{ \log_2 \left(1 + \text{SNR } h_{S,Q_r} \right), \log_2 \left(1 + \text{SNR } h_{Q_r,D} \right) \right\}. \quad (12)$$

The first term in Eq. (12) represents the maximum rate at which the relay can reliably decode the source message, while the second term in Eq. (12) represents the maximum rate at which the destination can reliably decode the message forwarded from relay. We note that such mutual information forms are typical of relay channel with full decoding at the relay [37]. The SNR threshold of this DF link for target rate B is given by $I_{DF_li} \geq B$ which is derived as

$$\text{SNR} \geq \frac{2^B - 1}{\min(h_{S,Q_r}, h_{Q_r,D})}. \quad (13)$$

In the proposed hybrid DF/AF cooperative transmission, we only consider that a relay can fully decode the signal transmitted over the source-relay link, but not the whole DF link, thus, the SNR threshold for the full decoding at the r -th relay reaches its lower bound as

$$\gamma_{th} \geq \frac{2^B - 1}{h_{S,Q_r}}. \quad (14)$$

For the DF protocol, let R denotes the number of the total relays, M denotes the set of participating relays, whose SNRs are above the SNR threshold, and the reliably decoding is available. The achievable channel capacity, C_{DF} , with SNR threshold is calculated as

$$C_{DF} = \sum_M \frac{1}{R} \mathbf{E}(\log_2(1 + y|M)) \Pr(M), \quad (15)$$

where $\mathbf{E}(\cdot)$ denotes the expectation operator, $y|M = (R - K)\gamma_{S,D} + \sum_{Q \in M} \gamma_{Q,D}$ denotes the instantaneous received SNR at the destination given set M with K participating relays, where $\gamma_{n,m}$ denotes the instantaneous received SNR at node m , which is directly transmitted from n to m . Since $y|M$ is the weighted sum of independent exponential random variables [38], the probability density function (PDF) of $y|M$ can be obtained using its moment generating function (MGF) and partial fraction technique for evaluation of the inverse Laplace transform, see Eq. (8d) and Eq. (8e) in paper [38]. $\Pr(M)$ in Eq. (15) is the probability of a particular set of participating relays which are obtained as

$$\Pr(M) = \prod_{Q \in M} \exp\left(-\frac{R\gamma_{th}}{\Gamma_{S,Q \in M}}\right) \prod_{Q \notin M} \left(1 - \exp\left(-\frac{R\gamma_{th}}{\Gamma_{S,Q \notin M}}\right)\right), \quad (16)$$

where $\Gamma_{u,v}$ denotes the average SNR over the link between nodes u and v .

Combining Eq. (11), Eq. (15) and Eq. (16) with the inequality $I_{DF_co} \leq C_{DF}$, since the maximum average mutual information, I , is upper bound by the achievable channel capacity, C , we can calculate the upper bound of SNR threshold γ_{th} for fully decoding in the DF protocol.

Now, we can obtain the upper bound and the lower bound of the SNR threshold γ_{th} for hybrid DF/AF cooperation. However, compared to the upper bound, the lower bound as shown in the Eq. (14) is more crucial for improving the transmission performance. This is

because the DF protocol plays a dominant role in the hybrid cooperation strategy, and accordingly we want to find the lower bound which provides as much as possible DF relays. We will elaborate this issue later. Fully decoding check can also be guaranteed by employing the error detection code, such as cyclic redundancy check. However, it will increase the system complexity [39].

3.3. Error probability for hybrid DF/AF cooperative transmission

In the maximum ratio combining the transmitted signal from R cooperative relays nodes, which underwent independent identically distributed Rayleigh fading, and forwarded to the destination node are combined. In this case the SNR per bit per relay link γ_r has an exponential probability density function (PDF) with average SNR per bit $\bar{\gamma}$:

$$p_{\gamma_r}(\gamma_r) = \frac{1}{\bar{\gamma}} e^{-\gamma_r/\bar{\gamma}}. \quad (17)$$

Since the fading on the R paths is identical and mutually statistically independent, the SNR per bit of the combined SNR γ_c will have a Chi-square distribution with $2R$ degrees of freedom. The PDF $p_{\gamma_c}(\gamma_c)$ is

$$p_{\gamma_c}(\gamma_c) = \frac{1}{(R-1)!\bar{\gamma}_c^R} \gamma_c^{R-1} e^{-\gamma_c/\bar{\gamma}_c}, \quad (18)$$

where $\bar{\gamma}_c$ is the average SNR per channel, then by integrating the conditional error probability over $\bar{\gamma}_c$, the average probability of error P_e can be obtained as

$$P_e = \int_0^\infty \hat{Q}(\sqrt{2g\gamma_c}) p_{\gamma_c}(\gamma_c) d\gamma_c, \quad (19)$$

where $g = 1$ for coherent Binary Phase Shift Keying (BPSK), $g = 1/2$ for coherent orthogonal BFSK, $g = 0.715$ for coherent BFSK with minimum correlation, and $\hat{Q}(\cdot)$ is the Gaussian Q -function, i.e., $\hat{Q}(x) = 1/\sqrt{2\pi} \int_x^\infty \exp(-t^2/2) dt$. For the BPSK case, the average probability of error can be found in the closed form by successive integration by parts, i.e.,

$$P_e = \left(\frac{1-\mu}{2}\right)^R \sum_{k=0}^{R-1} \binom{R-1+k}{k} \left(\frac{1+\mu}{2}\right)^R, \quad (20)$$

where

$$\mu = \sqrt{\frac{\bar{\gamma}_c}{1+\bar{\gamma}_c}}. \quad (21)$$

In the hybrid DF/AF cooperative network with two hops in each AF relay, the average SNR per channel $\bar{\gamma}_c$ can be approximately derived as

$$\bar{\gamma}_c = \frac{\gamma_h}{K + 2 \times J}, \quad (22)$$

where K and J are the numbers of the DF relays and AF relays, respectively. γ_h can be obtained from Eq. (6). In the DF protocol, due to the reliable detection, we can only consider the last hops, or the channels between the relay nodes and destination node.

As the average probability of error P_e is a precise indication for the transmission performance, we consequently propose a dynamic optimal combination strategy for the hybrid DF/AF cooperative transmission. In this algorithm the proper AF relays are selected to make P_e reach maximum.

First of all, like aforementioned procedure, relays are reordered according to the descending order of the SNR between source and relays, as shown in the Fig. 2. According to the proposed SNR threshold, we pick up the DF relays having SNR greater than threshold. Then, we proceed with the AF relay selection scheme, where the inappropriate AF relays are removed. The whole dynamic optimal combination strategy for the hybrid DF/AF cooperation is shown in the flow chart of Fig. 3.

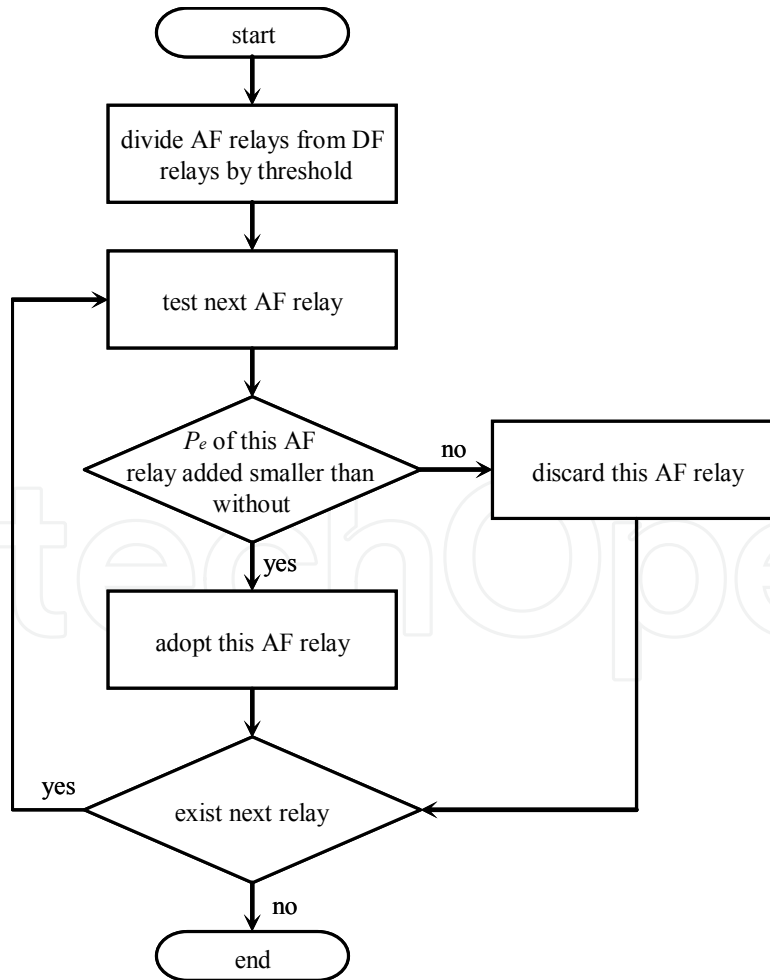


Figure 3. Flow chart of the dynamic optimal combination strategy for the hybrid DF/AF cooperation

4. Cooperative wavelet communication scheme

In this section, by taking advantage of the MRC property of the above mentioned multi-scale and multi-lag wideband channel and wavelet transceiver model, we consider a wideband cooperative wavelet communication scheme as shown in Fig. 4 [40], where we transmit data from source node S to destination node D through R DF relays, without the direct link between S and D .

We only consider and illustrate DF relay case; it is because only DF relays strictly fulfill the MRC property. The hybrid DF/AF scheme can approximately fulfill the MRC property and with some errors. This can be shown by the simulation results as well. If error requirement is not very demanding, the relay selection strategy for DF relay case can easily extended for the hybrid DF/AF case.

Different relays operate at different frequency bands and all relay links undergo multi-scale and multi-lag wideband channel. We assume that the channels are well known at the corresponding receiver sides. All the AWGN terms have equal variance N_0 . Relays are re-ordered according to the descending order of the (Signal to Noise Ratio) SNR between S and Q , i.e., $\text{SNR}_{SQ_1} > \dots > \text{SNR}_{SQ_R}$, where SNR_{SQ_r} denotes the r -th largest SNR between S and Q .

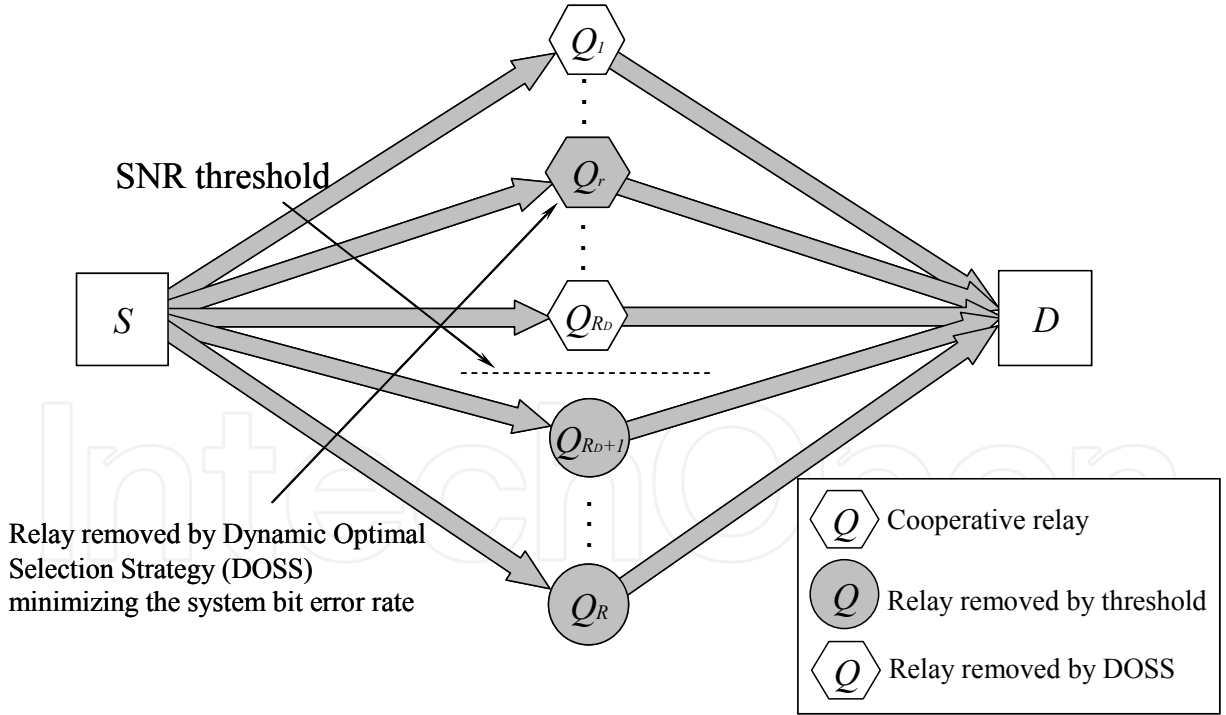


Figure 4. Cooperative wavelet communication scheme with dynamic optimal selection of DF relays in wideband multi-scale and multi-lag channel (S : Source, D : Destination, Q_r : r -th Relay).

In this model, relays can determine whether the received signals are decoded correctly or not, just simply compare its received SNR to the threshold. The SNR threshold for the full decoding at the r -th relay reaches its lower bound as

$$\gamma_{th} \geq \frac{2^B - 1}{h_{s,Q_r}}, \quad (23)$$

where B is the target rate of link between source node and relay, and h_{s,Q_r} denotes the power gain of the channel from source node to the r -th relay. Therefore, the relays with SNR below the threshold will be removed first, as shown with the gray circles in Fig. 4. The other R_D relays shown with hexagons are DF relays. According to the dynamic optimal selection strategy, which will be proposed in the next section, we select proper DF relays for cooperation. A one bit feedback channel from destination to relay is used for removing the unsuitable DF relays.

Haar wavelet signaling is adopted in the cooperative wideband system to transfer the multi-scale and multi-lag channel into the total M_D flat-fading channels

$$M_D = \sum_{r=1}^{R_D} \sum_{m=M_{Q_r,0}}^{M_{Q_r,1}} (L(m)), \quad (24)$$

where $L(m)$ denotes the number of the multilag for corresponding scaling index m , for the Doppler scale index m with spread $M_{Q_r,1} - M_{Q_r,0}$, at r -th cooperative link. For capturing the multi-scale and multi-lag diversity in the wideband channel, other wavelets, such as Daubechielkhs wavelets, Symlets, etc., have the same capability, since they all possess orthogonality in both scale and lag domain. Rational orthogonal wavelets can be adopted for the scale factor of a_0^m , $1 \leq a_0 \leq 2$, which is more suitable for the practical scenario [34]. However, wavelet selection problem is beyond the scope of this thesis. In this chapter, we focus on the multi-relay, multi-scale, and multi-lag diversity issue of the cooperative wideband system.

5. Dynamic optimal relay selection strategy

In the maximum ratio combining, the transmitted signal from R_D cooperative relays nodes over all multi-scale and multi-lag channel, which underwent independent identically distributed (i.i.d.) complex Gaussian fading, are forwarded to the destination node and combined. In this case, the average probability of error can be found in the closed form as

$$P_e = \left(\frac{1-\mu}{2} \right)^{M_D} \sum_{k=0}^{M_D-1} \binom{M_D-1+k}{k} \left(\frac{1+\mu}{2} \right)^{M_D}, \quad (25)$$

where

$$\mu = \sqrt{\frac{\bar{\gamma}_c}{1 + \bar{\gamma}_c}}, \quad (26)$$

In the proposed DF cooperative wideband network, because of the fully decoding at the relays, we only consider the link between relays and destination. Therefore, the average SNR per channel $\bar{\gamma}_c$ can be derived as

$$\bar{\gamma}_c = \left(\prod_{Q_r \in \text{DF}} \prod_{m=M_{Q_r,0}}^{M_{Q_r,1}} \prod_{l=0}^{L(m)} \frac{E_Q h_{Q_r,D}(m,l)}{N_o} \right)^{1/M_D}, \quad (27)$$

where $h_{Q_r,D}(m,l)$ denotes the power gains corresponding to the m -th scale and l -th lag, of the channel from the r -th relay to the destination in DF protocol. Combining Eq. (25), (26) and (27), we derive the analytical expression of the BER performance for the proposed DF cooperative wideband network.

As the average probability of error P_e is a precise indication, we can use it to predict the comprehensive transmission performance, only given the channel gains and SNRs at the destination. Consequently, we propose a dynamic optimal selection strategy for the cooperative multi-scale and multi-lag communications. In this algorithm the proper relays are selected to make P_e reach the minimum. First of all, relays are ordered according to the descending order of the SNR between source and relays, as shown in the Fig. 4. According to the proposed SNR threshold, we pick up the DF relays whose SNR is above the threshold.

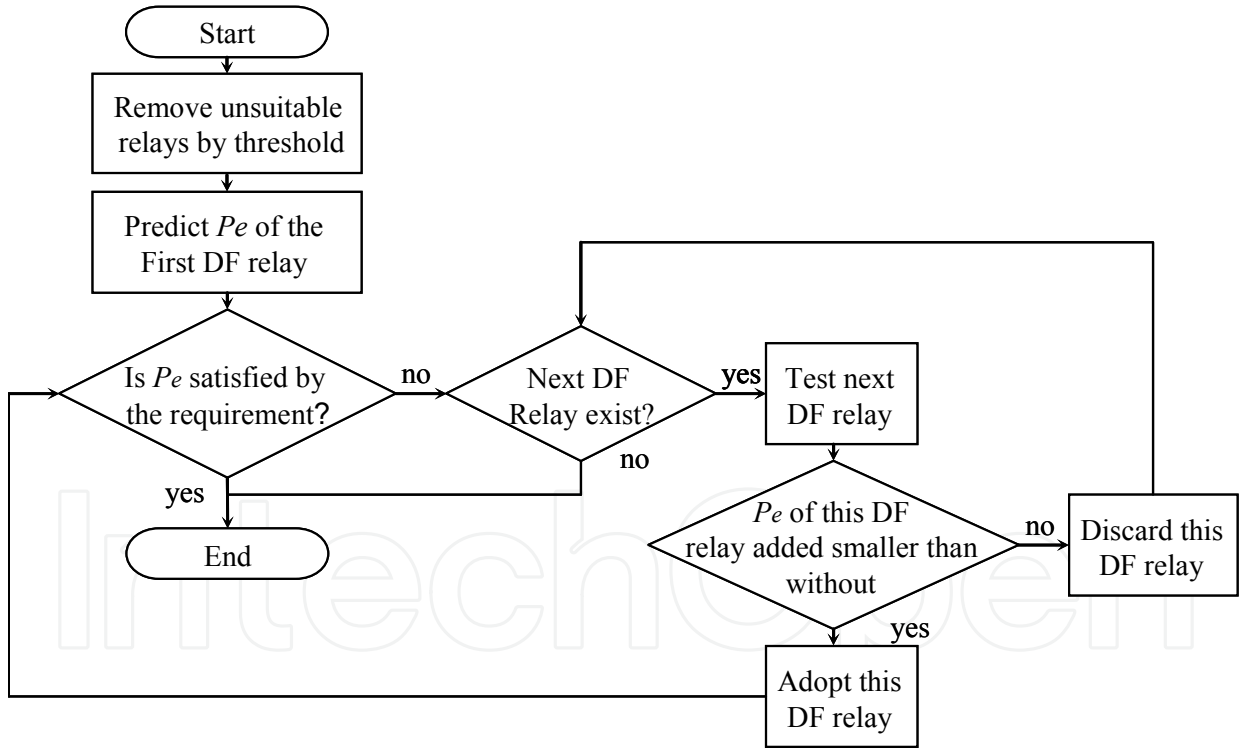


Figure 5. Flow chart of the dynamic optimal selection strategy for the cooperative wideband communications

Then, we proceed with the relay selection to maximize the entire BER performance and try to satisfy the P_e requirement, where the inappropriate DF relays are removed. The whole dynamic optimal selection strategy for the cooperative wideband communication is shown in the flow chart of Fig. 5.

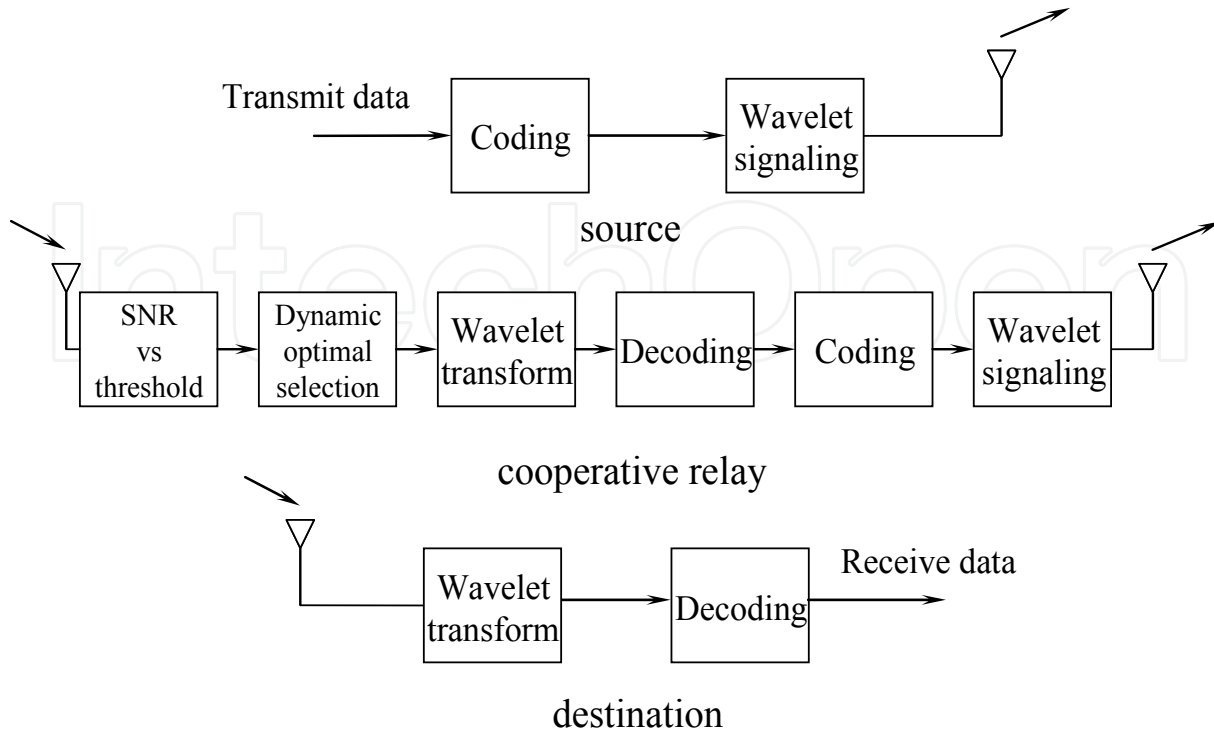


Figure 6. Relay selection in the cooperative wavelet wideband wireless transmission strategy (top: source, middle: cooperative relay, bottom: destination)

The wavelet signaling and transceiver design are shown in the Fig. 6. Before the transmission, Haar wavelet signaling is adopted to capture the multi-scale and multi-lag diversity in the wideband channel. In the relaying section, we first remove un-decodable relays by SNR threshold. Then, those relays which undergo the deep fading between relay-destination links will be removed by using the dynamic optimal selection strategy, in order to meet the P_e requirement. After recoding again, Haar wavelet signaling is applied again on the signal. At the destination node, after inverse wavelet transformation, the resulting signals are used for the combination and detection.

6. Simulation results and analysis

Test Case 1 (BER performance based Relay selection for cooperative communications):

In this example, first, we simulated BPSK modulation, Rayleigh channel, flat fading, without OFDM, and supposed the SNR threshold for correct decoding is $4E_b/N_0$, then we assumed $h_{Q_i,D} = h_{S,Q_j} = h_{Q_j,D} = 1$, for all branches, to verify proposed analytical BER expression. The resulting average BER were plotted against the transmit SNR defined as $\text{SNR} = E_b/N_0$. As shown in the Fig. 7, the theoretical curves of multi-DF cooperation derived from our analytical closed-form BER expression clearly agree with the Monte Carlo simulated curves, while the theoretical curves of 2-AF and 3-AF cooperation match the simulation result only at the low SNR region.

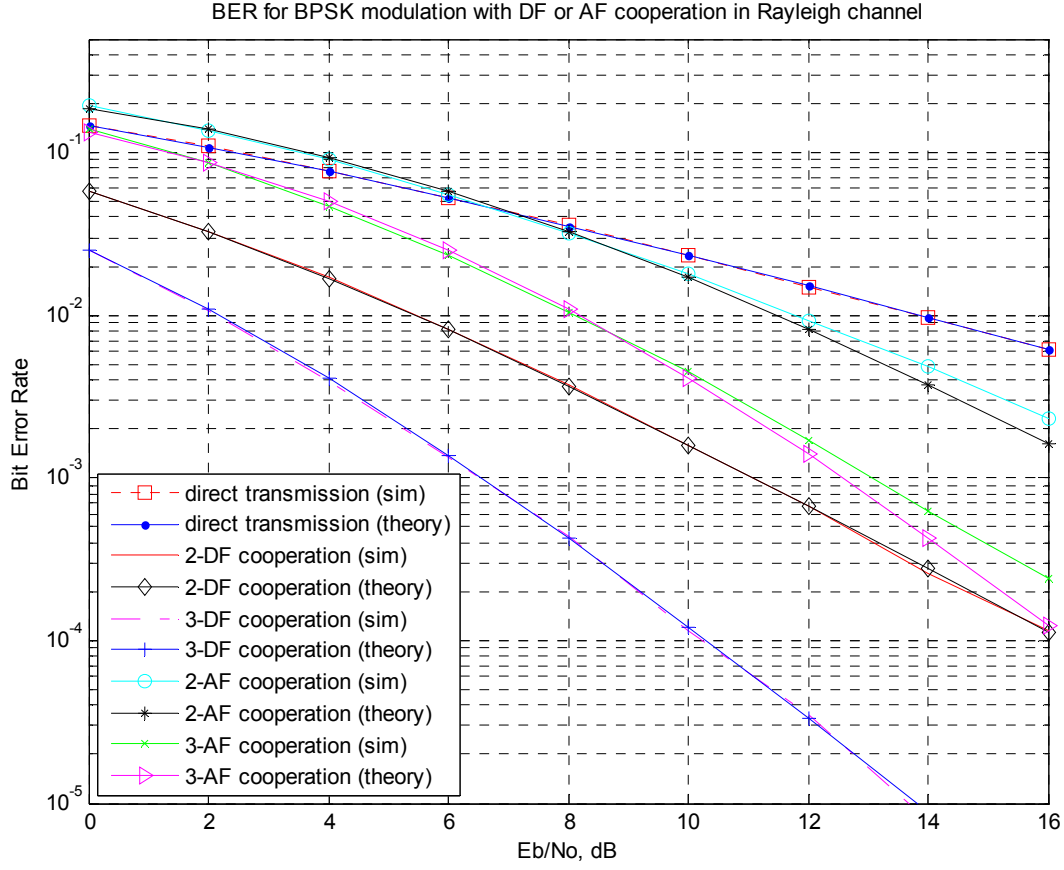


Figure 7. BER performance for DF or AF cooperation.

Fig. 8 shows the BER performance for hybrid DF-AF cooperation. For the DF-dominant hybrid cooperation, the theoretical curves exhibit a good match with the Monte Carlo simulation results curves. The slight gap between theoretical and simulation BER results for the hybrid case of 1-DF + multi-AF can be explained by the AF relay fading which was considered as a double Gaussian channel, a product of two complex Gaussian channel [49]. Obviously, the distribution of combined SNR (i.e., γ_c) will no longer follow the chi-square distribution giving rise to this slight difference.

Comparing 2-DF to 2-AF in Fig. 7, or 2-DF plus 1-AF to 1-DF plus 2-AF in Fig. 8, or other hybrid DF-AF protocols with the same R , we can see that the fully decoded DF protocols always show a better BER performance than AF protocols. Therefore, DF protocols with a reliable decoding play a more important role in hybrid cooperative networks than AF protocols. Meanwhile, we can see from the figure that, changing to the AF scheme for the relay nodes with SNR below the threshold also improves the BER performance, as well as the diversity gain of the whole network. In fact, this is a better way than just discarding these relay nodes.

Test Case 2 (Relay selection for cooperative communications over multi-scale and multi-lag wireless channels):

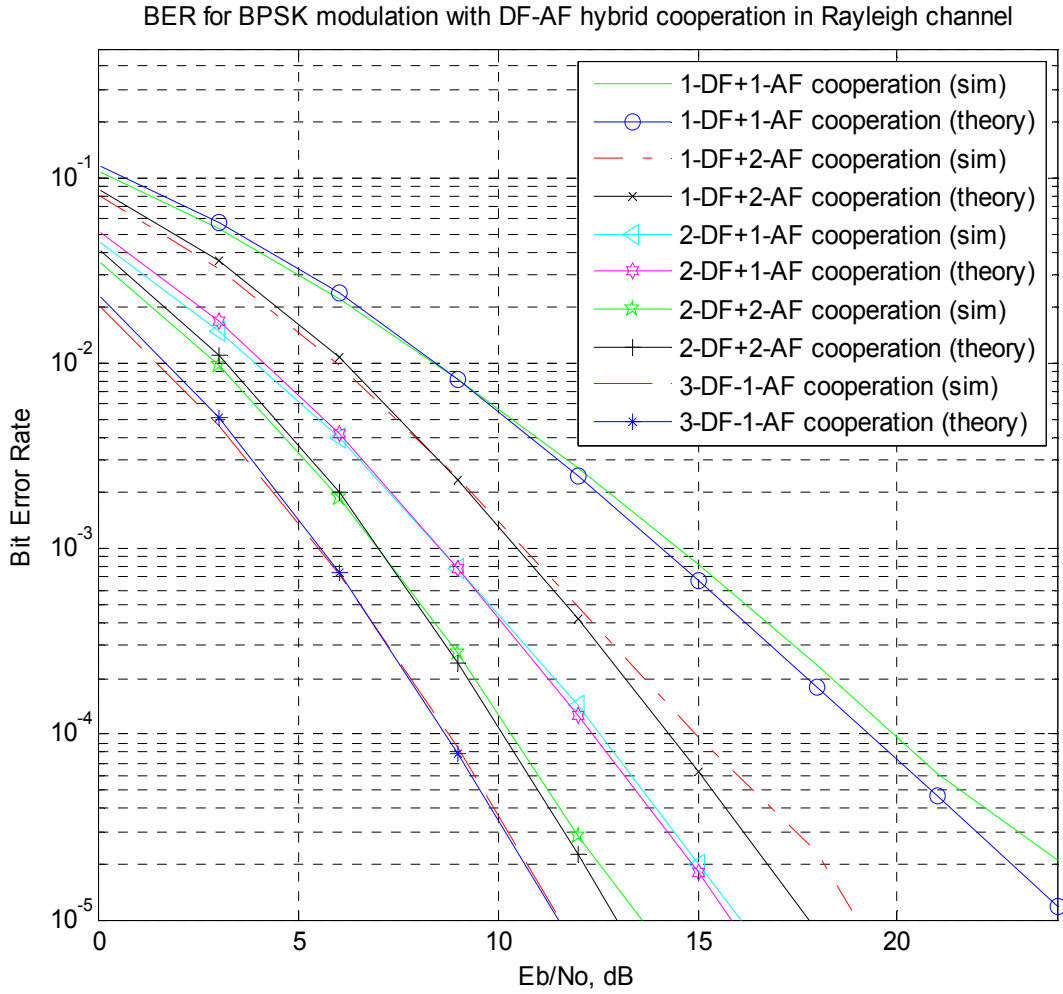


Figure 8. BER performance for hybrid DF+AF cooperation.

In this case, we use the simulation results to verify our theoretical claims on the analytical BER expression and illustrate the dynamic optimal selection strategy.

In the first example, simulation results justify the proposed analytical BER expression for cooperative wavelet communications with multi-scale and multi-lag wireless channel, i.e., the combination of Eq. (25), (26) and (27), which can be used to predict the transmission performance and enable the dynamic optimal selection strategy as shown in the Fig. 5. BPSK is adopted as the modulation scheme, and the 2-decomposition level Haar wavelet transform is adopted as a RAKE receiver to capture the multi-scale and multi-lag diversity components, and transfer the multi-relay, multi-scale and multi-lag channel into the orthogonal flat-fading channels. Therefore, we consider 2-relay three orthogonal channels in this simulation. Relay 1 has 1-scale and 2-lag diversity components, the power gains are $h_1 = 4$ and $h_2 = 1$. Relay 2 has 1-scale and 1-lag diversity component, the power gain is $h_3 = 1$. The resulting average BER are plotted against the transmit SNR defined as $\text{SNR} = E_b/N_0$. As shown in the Fig. 9, the theoretical curves of different diversities derived

from our analytical closed-form BER expression clearly agree with the Monte Carlo simulated curves.

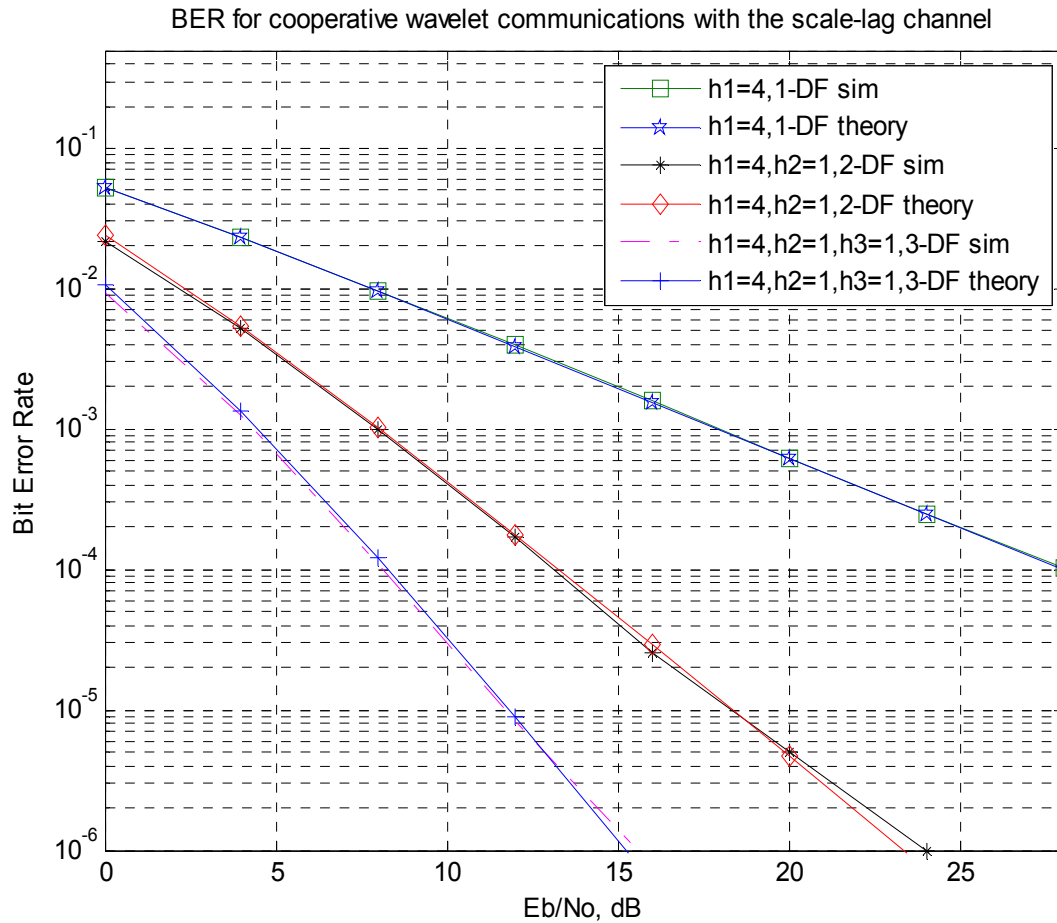


Figure 9. BER performance for cooperative wavelet wideband communications

In the second example, we illustrate how to exploit the proposed analytical BER expression together with dynamic optimal selection strategy to select relays for the cooperative wideband communications. We suppose the target P_e at SNR $E_b/N_o = 10\text{dB}$ is 10^{-4} . In the original state, we suppose that we already have 1-Relay with 1-scale and 2-lag diversity components, with power gains $h_1 = 4$ and $h_2 = 1$. The BER performance is shown by the triangle marked curve in Fig. 10. The P_e requirement is not met by the original state, so we expect to cooperate with more relays, to gain from more diversity components. For the test case 1, we test and combine with a deep fading relay with only one scale-lag diversity, power gain $h_3 = 0.04$. Analytical BER expression predicts that adding this deep fading relay deteriorates the BER performance. Therefore, we discard this relay. For the test case 2, we

test and combine with a relay with one scale-lag diversity, power gain $h_3 = 4$, which improves the BER performance, and satisfies the P_e requirement. Therefore, we adopt this relay.

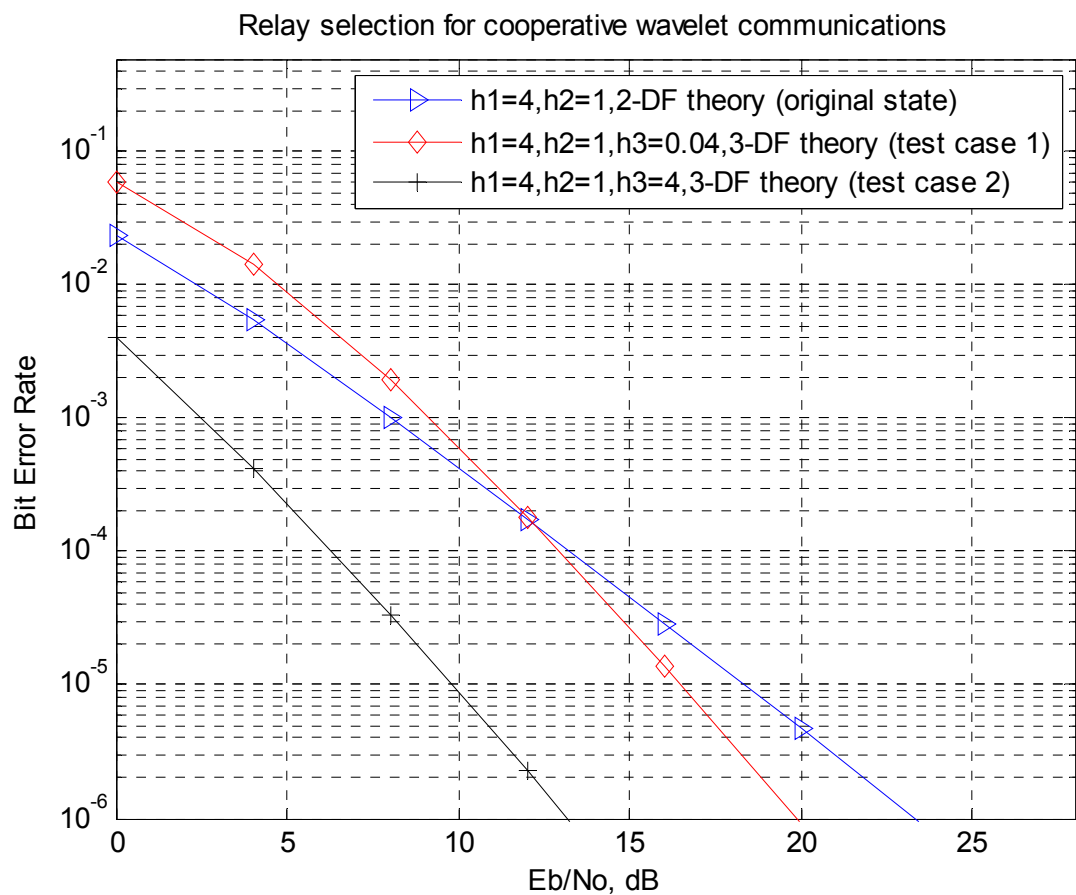


Figure 10. Relay selection for cooperative 2-decomposition level wavelet wideband communication

7. Conclusions

Wideband scale-lag channels can be found in many applications, including ultra-wideband communications and underwater acoustic communications. Signaling and reception schemes using the wavelet theory enable the multi-scale and multi-lag diversity in the wideband system. In this chapter, we designed a cooperative wavelet system to capture the joint cooperative-scale-lag diversity. We proposed the analytical BER expression for the cooperative wavelet wideband communication. The agreement between the analytical

curves and numerical simulated results shows that the derived analytical BER expression is suitable for the performance prediction of cooperation wavelet wideband communication. The compact and closed-form BER expression can easily provide an insight into the results as well as a heuristic help for the design of future cooperative wavelet wideband systems. For the suggested cooperative wavelet protocol, we also presented a dynamic optimal selection strategy for the optimal relay selection, which maximizes the whole system transmission performance.

Author details

H. Lu and H. Nikookar

*International Research Centre for Telecommunications and Radar (IRCTR),
Dept. EEMCS, Delft University of Technology, Delft,
The Netherlands*

T. Xu

*Circuits and Systems Group (CAS),
Dept. EEMCS, Delft University of Technology, Delft,
The Netherlands*

8. References

- [1] Barbarossa S., *Multiantenna Wireless Communication Systems*, Norwood, MA: Artech House, 2005.
- [2] Foschini G. J. & Gans M., On the limits of wireless communication in a fading environment when using multiple antennas, *Wireless Personal Commun.*, vol. 6, Mar. 1998, pp. 311-335.
- [3] Laneman J. N., Cooperative diversity in wireless networks: algorithm and architectures, *Ph.D. dissertation*, MIT. Cambridge, MA, Sep. 2002.
- [4] Sendonaris A., Erkip E., & Aazhang B., User cooperation diversity—Part I: System description, *IEEE Trans. Commun.*, vol. 51, no. 11, Nov. 2003, pp. 1927–1938.
- [5] Sendonaris A., Erkip E. & Aazhang B., User cooperation diversity—Part II: Implementation aspects and performance analysis, *IEEE Trans. Commun.*, vol. 51, no. 11, Nov. 2003, pp. 1939–1948.
- [6] Liu K. J. R., Sadek A. K., Su W. & Kwasinski A., *Cooperative Communications and Networks*, Cambridge University Press, 2009
- [7] Federal Communications Commission, Revision of part 15 of the commission's rules regarding ultra-wideband transmission systems, First report and order, ET Docket 98-153, FCC 02-48, Feb. 14, 2002, pp. 1–118.
- [8] Sayeed A. M. & Aazhang B., Joint multipath-Doppler diversity in mobile wireless communications. *IEEE T. Commun.*, vol. 47, no. 1, 1999, pp. 123–132.

- [9] Rickard S., Balan R., Poor V. & Verdu S., Canonical time-frequency, time-scale, and frequency-scale representations of time-varying channels. *J. Comm. Infor. Syst.*, vol. 5, no. 5, 2005, pp. 1–30.
- [10] Jiang Y. & Papandreou-Suppappola A., Discrete time-scale characterization of wideband time-varying systems. *IEEE T. Signal. Proces.*, vol. 54, no. 4, 2006, pp. 1364–1375.
- [11] Margetts A. R., Schniter P., and Swami A., Joint scale-lag diversity in wideband mobile direct sequence spread spectrum systems. *IEEE T. Wirel. Commun.*, vol. 6, no. 12, 2007, pp. 4308–4319.
- [12] Xu T., Leus G. & Mitra U., Orthogonal wavelet division multiplexing for wideband time-varying channels. *Proc. of IEEE ICASSP*, Prague (Czech Republic), May 2011, pp. 3556–3559.
- [13] Leus G., Xu T. & Mitra U., Block Transmission over Multi-Scale Multi-Lag Wireless Channels. *Proc. of the Asilomar Conference on Signals, Systems, and Computers*, Pacific Grove, California, USA, Nov. 2010.
- [14] Rickard S., Time-frequency and time-scale representations of doubly spread channels, *Ph.D. dissertation*, Applied and Computational Mathematics Dept., Princeton Univ., Princeton, NJ, Nov. 2003
- [15] Bircan A., Tekinay S. & Akansu A., Time-frequency and time-scale representation of wireless communication channels, *Proc. of IEEE Int. Symp. Time-Frequency/Time-Scale Analysis*, Pittsburgh, PA, Oct. 1998, pp. 373–376
- [16] Capoglu I. R., Li Y. & Swami A., Effect of doppler spread in OFDM based UWB systems, *IEEE Transactions on Wireless Communications*, vol. 4, no. 5, Sep. 2005, pp. 2559–2567.
- [17] Zhang H., Fan H. H. & Lindsey A., A wavelet packet based model for time-varying wireless communication channels, *Proc. of IEEE Workshop Signal Processing Advances Wireless Communications*, Mar. 2001, pp. 50–53.
- [18] Johnson M., Freitag L. & Stojanovic M., Improved Doppler tracking and correction for underwater acoustic communications, *Proc. of IEEE Int. Conf. Acoustic, Speech, Signal Processing*, vol. 1, Germany, Apr. 1997, pp. 575–578
- [19] Sharif B. S., Neasham J., Hinton O. R. & Adams A. E., A computationally efficient Doppler compensation system for underwater acoustic communications, *IEEE J. Oceanic Eng.*, vol. 25, no. 1, Jan. 2000, pp. 52–61.
- [20] Mitra U. & Leus G., Equalizers for multi-scale / multi-lag wireless channels, *Proc. of IEEE Global Telecommunications Conference*, 2010. pp. 1–5.
- [21] Acosta G., Tokuda K. & Ingram M. A., Measured joint Doppler-delay power profiles for vehicle-to-vehicle communications at 2.4 GHz, *Proc. of IEEE Global Telecommunications Conference*, 2004. pp. 3813–3817.
- [22] Acosta G. & Ingram M. A., Six time- and frequency-selective empirical channel models for vehicular wireless LANs, *Proc. of 1st IEEE International Symposium on Wireless Vehicular Communications*, September 2007.

- [23] Blahut R. E., Miller W. Jr. & Wilcox C. H., Eds., *Radar and Sonar, Part I, IMA Volumes in Mathematics and its Applications*. New York: Springer-Verlag, 1991.
- [24] Weiss L. G., Wavelets and wideband correlation processing, *IEEE Signal Process. Mag.*, vol. 11, no. 1, Jan. 1994, pp. 13–32.
- [25] Young R. K., *Wavelet Theory and Its Applications*. Norwell, MA: Kluwer, 1993.
- [26] Tsatsanis M. K. & Giannakis G. B., Time-varying system identification and model validation using wavelets, *IEEE Trans. Signal Process.*, vol. 41, no. 12, Dec. 1993, pp. 3512–3523.
- [27] Iverson D. E., Coherent processing of ultra-wide-band radar signals, *Proc. Inst. Elect. Eng. Radar, Sonar, Navigation*, vol. 141, Jun. 1994, pp. 171–179.
- [28] Sharif B. S., Neasham J., Hinton O. R. & Adams A. E., A computationally efficient Doppler compensation system for underwater acoustic communications, *IEEE J. Oceanic Eng.*, vol. 25, no. 1, Jan. 2000, pp. 52–61.
- [29] Wornell G.W., Emerging applications of multirate signal processing and wavelets in digital communications, *Proc. of IEEE*, vol. 84, Apr. 1996, pp. 586–603.
- [30] Leus G. & van Walree P., Multiband OFDM for covert acoustic communications, *IEEE J. Sel. Area. Comm.*, vol. 26, no. 9, 2008, pp. 1662–1673.
- [31] Li B., Zhou S., Stojanovic M., Freitag L. & Willett P., Multicarrier communication over underwater acoustic channels with nonuniform doppler shifts, *IEEE J. Oceanic. Eng.*, vol. 33, no. 2, 2008, pp. 198–209.
- [32] Martone M., Wavelet-based separating kernels for array processing of cellular ds/cdma signals in fast fading, *IEEE T. Commun.*, vol. 48, no. 6, 2000, pp. 979–995.
- [33] Mitra U. & Leus G., Equalizers for multi-scale / multi-lag wireless channels, *Proc. of IEEE Global Telecommunications Conference, 2010*. pp. 1–5.
- [34] Yu L. & White L. B., Optimum receiver design for broadband Doppler compensation in multipath/doppler channels with rational orthogonal wavelet signaling, *IEEE T. Signal. Proces.*, vol. 55, no. 8, 2007, pp. 4091–4103.
- [35] Linfoot S. L., Ibrahim M. K. & Al-Akaidi M. M., Orthogonal wavelet division multiplex: An alternative to ofdm, *IEEE T Consum. Electr.*, vol. 53, no. 2, 2007, pp. 278–284.
- [36] Lu H., Nikookar H. & Lian X., Performance evaluation of hybrid DF-AF OFDM cooperation in Rayleigh Channel, *Proc. of European Wireless Technology Conference*, Sep. 2010, Paris, France.
- [37] Cover T. M. & El Gamal, A. A. Capacity theorems for the relay channel, *IEEE Trans. Inform. Theory*, vol. 25, no. 5, Sep. 1979, pp. 572–584.
- [38] Farhadi G. & Beaulieu N. C., On the Ergodic Capacity of Wireless Relaying System over Rayleigh Fading Channels, *IEEE Trans. Wireless Communications*, vol. 7, no. 11, Nov. 2008, pp. 4462–4467.
- [39] Lin S. & Constello D. J., *Error Control Coding: Fundamentals and Applications*. Englewood Cliffs, NJ: Prentice–Hall, 1983.

- [40] Lu H., Xu T., Lakshmanan M. and Nikookar H., Cooperative wavelet communication for multi-relay, multi-scale and multi-lag wireless channels, *Proc. of IEEE Vehicular Technology Conference (VTC)*, Budapest, Hungary, May, 2011, pp. 1-5.

IntechOpen

IntechOpen